

Kinetic regularities of solid-phase formation in the branching chain reaction of dichlorosilane oxidation in rf plasma at low pressures and 293 K

Nikolai M. Rubtsov,* Georgii I. Tsvetkov and Victor I. Chernysh

Institute of Structural Macrokinetics and Materials Science, Russian Academy of Sciences, 142432 Chernogolovka, Moscow Region, Russian Federation. E-mail: ab3590@mail.sitk.ru

DOI: 10.1070/MC2006v016n01ABEH002176

In studies of the initiated ignition of dichlorosilane–oxygen mixtures it has been shown that rf discharge applied before ignition leads to an increase in the lifetime of aerosol particles in the reactor volume, in contrast to direct current discharge which markedly decreases the amount of aerosol particles formed in ignition. Ordered structures of the type of ‘liquid dust crystal’ have been detected in rf plasma of branching-chain heterophaseous reaction.

Dust particles immersed within a plasma environment, such as those in protostellar clouds, planetary rings or cometary environments, will acquire an electric charge. In semiconductor technology, particles can grow in the plasmas in surface processing reactors, and remain electrically suspended there until they fall to a surface and contaminate it,¹ which is undesirable. On the other hand, the occurrence of ordered structures in dusty plasma may be used in nanotechnology.²

Colloidal plasmas can be defined as dusty plasmas in which dust cannot longer be considered a contaminant but should instead be considered an integral component of the plasma. Structures called Coulomb crystals can form within colloidal plasmas, once certain criteria are met.¹ If the ratio of the inter-particle potential energy to the average kinetic energy is high enough the particles form either a ‘liquid’ structure with short-range ordering or a ‘crystalline’ structure with long-range ordering.

Most previous experiments have employed monodisperse spheres to form Coulomb crystals.³ However, in nature (as well as in most plasma processing environments) the distribution of particle sizes is randomised and disperse. It has been shown that, while monodisperse particles form ‘solid’ Coulomb crystals, a Gaussian distribution of particles forms ‘liquid’ Coulomb crystals instead.⁴

For the most part, the experiments on ‘dust crystals’ have been carried out using artificial particles of a given size. The behaviour of the particles being directly relevant to a gaseous chemical reaction, as well as the behaviour of the system of growing particles in dust plasma, was investigated using plasma-

enhanced SiH₄ and CH₄ pyrolysis.^{5,6} Regular structures of SiO₂ aerosol particles were obtained in Ar plasma; however, the reaction of SiH₄ oxidation was used only for the synthesis of the aerosol.⁷

From the literature data it transpires that kinetical features of phase formation in rf plasma in a heterophaseous branching chain process (BCP) like SiH₄ oxidation during ignition and immediately after it have not been studied, though such investigations can provide additional data on the phase formation in BCP.

The oxidation of SiH₄ and its derivatives can be used for both the production of nanosized particles⁸ and thin film deposition being of practical value either in integrated circuits processing or as selective membranes in semiconductor sensors.⁹ The BCPs are quite suitable for investigation into the physics of complex plasma because the ignition in these is accompanied by the generation of charged particles in reactions of recombination of active species formed during combustion on the surface of SiO₂ aerosol.^{10,11} It means that dusty plasma occurs during ignition even without external energy source. It was shown that a constant electrical field even without discharge influences on the lower limit of self-ignition and chemical oscillations in the reaction of oxidation of dichlorosilane (DCS).¹² It was also shown that the constant electrical field in the absence of a discharge applied before ignition causes a decrease in the amount of SiO₂ aerosol formed in ignition; in this case, the features of the flux formed by charged particles determine the thickness and texture of the SiO₂ film deposited.^{10,13} For instance, the rate of deposition on a negatively charged electrode is about four times higher than

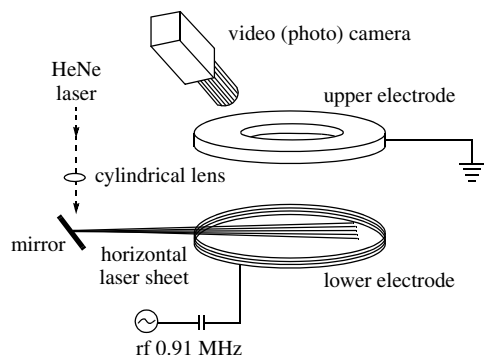


Figure 1 Experimental cell for visualising of aerosol particles.

that on a positively charged one. This indicates the significant role of positive ions. Being applied after ignition, a constant electric field does not influence the aerosol.¹⁰

Based on the phenomena, the method of thin film deposition at room temperature in a decaying flame was devised.¹⁴ The method provides complete elimination of aerosol incorporation into the film deposited. The reactor equipped with an instrumental cell for creation of glow discharge under low pressure and wafer holders was used. The glow discharge area was located in the cell in the way that the wafers were placed outside it during the deposition and were therefore proofed against radiation damage. The discharge was sustained by the own conductivity of BCP (discharge current of $\sim 5 \mu\text{A}$). The aerosol particles were captured by an electrical field, and they did not reach the wafers during the process.

However, the behaviour of aerosol plasma flux of SiO_2 formed in an electrical field has not been investigated, in particular, by means of visualising. One can expect the formation of ordered structures of aerosol particles in plasma of BCP of silanes oxidation during ignition and immediately after it. Kinetic behaviour of such systems is complicated due to the growing of size-distributed particles in the combustion process.

The present work is aimed at the investigation of kinetic regularities of SiO_2 formation during the ignition of DCS–oxygen mixtures under rf plasma discharge.

Experiments were carried out in the vacuum setup described elsewhere.¹⁰ The experimental cell is shown schematically in Figure 1. The rf discharge was formed by applying a 0.91 MHz signal from a Tesla 004 rf generator capacitive coupled to the lower electrode of a parallel-plate reactor. The lower electrode is a copper disk 8 cm in diameter, while the upper is a copper ring, with inner and outer diameters of 3 and 8 cm, respectively. The electrode separation is 0.7 cm. In some instances, rf discharge was formed using a copper needle instead of an upper ring electrode mounted 3 cm above the centre of the lower electrode. The particle cloud was imaged using a horizontal sheet of He–Ne laser light ($\lambda = 632.8 \text{ nm}$) formed by means of a cylindrical lens along with $800\times$ video camera connected to a video recorder and a frame grabber, or $11\times 4 \text{ Mpixel}$ photo camera mounted above the top of the cell. The cell was mounted in a quartz cylinder 120 mm in diameter and height with a removable bottom. Experiments were conducted under static conditions at 300 K and a total pressure of 7–12 Torr. A prepared combustible mixture of 30% DCS + 30% O_2 + 40% Kr was fed into the reactor from a storage tank through a vacuum valve. The mixture was ignited either by heating a Nichrome wire 0.3 mm in diameter using a capacitor bank (3000 μF) or rf discharge. The optical window of the reactor (not shown in Figure 1) was repolished after every ten ignitions. The scattering of light at an angle of 90° by aerosol particles was also analysed as described elsewhere.¹⁵ The purity of DCS was checked by IR spectrophotometry.¹⁶

First, it has been shown that if rf discharge is used for initiation of ignition, the cloud of aerosol particles exists under our conditions up to 400 s. However, if rf discharge is applied after ignition, the cloud exists for $\sim 60 \text{ s}$, this time is also markedly longer than without rf discharge (see below). It means that rf

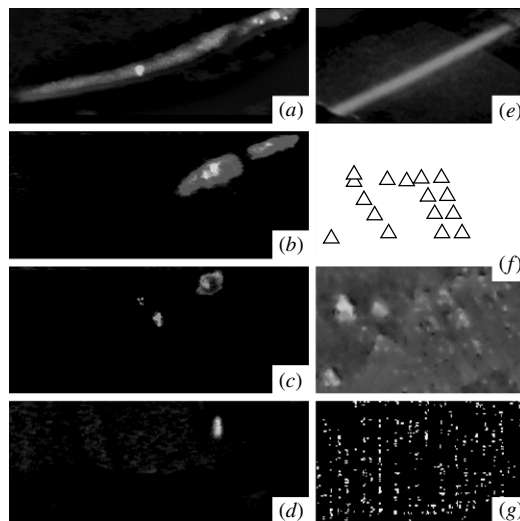


Figure 2 Images of aerosol cloud after ignition of 7 Torr 30% SiH_2Cl_2 + 30% O_2 + 40% Kr. (a) video image, (e) photo image, aerosol cloud in the absence of rf discharge; (b) video image, 6 s after switching on a rf discharge; (c) video image, (f) enlarged photo image (fragment) and its reconstruction, 15 s after switching on a rf discharge; aerosol cloud containing particles of triangle shape; (d) video image, (g) enlarged photo image (fragment), 60 s after switching on a rf discharge; long-lived aerosol cloud. Images (f) and (g) were obtained using laser sheet and computer processing.

discharge makes for the conservation of charge captured by SiO_2 particles during the ignition. By this means an alternating electrical field does not act similar to the constant electrical field¹⁰ applied before ignition. The behaviour of highlighted particles formed after initiated ignition and recorded using video/photo cameras is shown in Figure 2. In the absence of plasma, the scattering area of illuminated aerosol shown in Figure 2(a),(e) disappears gradually as a unit in a time $< 30 \text{ s}$ due to sedimentation over the pressures studied in agreement with our earlier results.¹⁵ Note that the range of pressures (7–12 Torr) was chosen because for the given combustion mixture at pressures lower than 7 Torr the amount of aerosol is too small for visual detection of particles; at higher pressures ($> 12 \text{ Torr}$) the inner reactor surface is rapidly covered with SiO_2 aerosol, the spurious reflection from it makes the recording difficult. In addition, the ignition at pressures $> 12 \text{ Torr}$ is accompanied by a characteristic sound. It means that a shock wave occurs; therefore, the fluxes produced can mix aerosol, preventing the appearance of ordered structures. In the presence of plasma aerosol particles move towards electrodes for 5–15 s [Figure 2(b),(c)]. The transitional process [Figure 2(b),(c)] is accompanied by the occurrence of an increasing hollow space in the centre of the cell (a void).¹ The process is also accompanied by the occurrence of high reflective crystallites of a triangle shape, which form ordered lamellar structures [Figure 2(f)]. These triangle particles can be seen only at certain angles; therefore, it was concluded that the particles

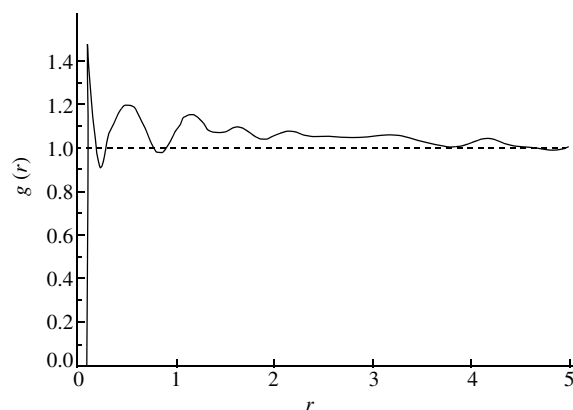


Figure 3 Pair correlation function for image in Figure 2(g).

were crystalline rather than amorphous. In a time of ~ 15 s after rf discharge is applied, only small particles remain in the volume. The particles form a toroidal cloud close to interelectrode distance; in this case, the cloud of aerosol exists between electrodes for about 20–400 s. The position and shape of the cloud in space do almost not undergo any changes during this time. Its illuminated part is shown in Figure 2(d). As is seen in Figure 2, the test system demonstrates an ordered behaviour in rf discharge. The process shown in Figure 2 is well reproducible.

The image of the long-lived aerosol cloud recorded using a laser sheet and a photo camera is shown in Figure 2(g). It is seen that the particles of different sizes form a lamellar structure. A pair correlation function (the probabilities of finding the centre of a particle within a given distance from the centre of another particle) calculated is shown in Figure 3. The function shown exhibits several distinct peaks. This indicates the existence of a certain degree of long-range correlation among the particles. Note that the pair correlation function calculated for Gaussian distributed 3–10 microns glass spheres in plasma⁴ showed the range ordering characteristic of ‘liquid’ Coulomb crystals. Therefore, in a similar way to ref. 4 the system of growing size-distributed particles exhibits the properties of ‘liquid’ dusty plasma. Actually the criterion condition of crystallization in terms of pair correlation function¹ is not fulfilled. According to the criterion, the ratio between maximal and minimal values of the function must exceed 0.2.

Let us roughly estimate the size of the particles observed. The initial photo seizes a part of the cell about 2×2 cm. There are ~ 2000 pixels in each dimension. Therefore, the resolution ratio of the optical system based on photo camera is ≥ 10 μm . The particles that form triangles [Figure 2(f)] are well resolved and appear as circles in the figure; thus, the upper limit of their size is of the order of 10 μm , and the size of triangle-shaped crystallites is ≤ 50 –70 μm . On the contrary, the particles in Figure 2(g) are not resolved and appear as rectangles. Thus, the particles comprising the long-lived aerosol cloud have size of the order of $\ll 10$ μm . This is in agreement with the experimentally determined distribution of SiO_2 particles in DCS oxidation.¹⁷

The behavior of aerosol particles strongly depends on the degree of inhomogeneity of rf plasma. The inhomogeneous discharge was produced using a needle instead of a ring electrode mounted 3 cm above the centre of a lower electrode. Under these conditions, the stable toroidal aerosol cloud occurs around the area of discharge [Figure 4(a)], in this case triangle-shaped particles move in parallel with a lower electrode in the direction of discharge in a helical manner. Under these conditions, triangle-shaped and small particles disappear simultaneously. The phenomenon can be observed for about 400 s. The action of rf plasma on the lower electrode leads to the inhomogeneous etching of a SiO_2 layer formed during the ignition. Etching figures have the similar shape and size as triangle-shaped crystallites being observed in the reactor volume [Figure 4(b)].

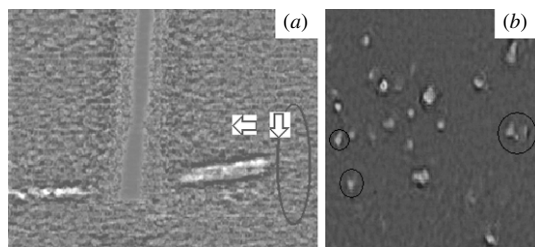


Figure 4 (a) A video image of the SiO_2 aerosol structure formed in inhomogeneous plasma. The area of rf discharge is a vertical column in the centre of the picture. The arrows show directions of the movement of highlighted aerosol particles. 9 Torr, 30% SiH_2Cl_2 + 30% O_2 + 40% Kr. (b) A photo image of highlighted surface of the lower electrode. A triangle shaped crystallite fallen from the volume is in the right upper corner of the picture. The figures selected in the image are etching ones.

Therefore, the crystallites comprise the constructional units of the film formed.

One of the main results of the work is the fact that an electrical field applied has a marked influence on the regularities of phase formation both during and after ignition in heterophaseous BCP. A correlation in the plasma of growing particles of SiO_2 formed in BCP of DCS oxidation has been experimentally observed for the first time. The macroscopic ordering of the system manifesting itself in void occurrence during transition processes in dust plasma was also detected. It has been shown that aerosol particles, undesirable in semiconductor technology applications, can be withdrawn from the reactor volume by applying either direct or alternative electrical field in the appropriate direction to wafers, being deposited.

This work was supported by the Russian Foundation for Basic Research (grant no. 05-03-33050a).

We are grateful to Professor O. F. Petrov (Institute for High Energy Densities of Joint Institute for High Temperatures RAS) for many useful discussions.

References

- 1 V. E. Fortov, A. G. Chrapak and I. T. Yakubov, *Fizika neideal'noi plazmy (Physics of non-ideal plasma)*, Fizmatlit, Moscow, 2004 (in Russian).
- 2 C. P. Poole and F. G. Owens, *Introduction to Nanotechnology*, Wiley, New York, 2003.
- 3 J. B. Pieper, J. Goree and R. A. Quinn, *J. Vac. Sci. Technol.*, 1996, **A14**, 519.
- 4 B. Smith, J. Vasut, T. Hyde, L. Matthews, J. Reay, M. Cook and J. Schmoke, *Adv. Space Res.*, 2004, **34**, 2379.
- 5 J. Perrin and Ch. Hollenstein, in *Dusty Plasmas: Physics, Chemistry and Technological Impacts in Plasma Processing*, ed. A. Bouchoule, Wiley, New York, 1999.
- 6 J. Gonzalez-Aguilar, I. Dème, L. Fulcheri, T. M. Gruenberger and B. P. Claude Daunesse, *Materials of E-MRS Spring Meeting 2002 SYMPOSIUM G TPP 7 Thermal Plasma Processes*, G-V.2.
- 7 I. Lin, C.-H. Chiang and W.-T. Jaun, *Chinese J. Phys.*, 1995, **33**, 453.
- 8 A. I. Gusev, *Usp. Fiz. Nauk*, 1998, **163**, 55 [*Physics-Uspekhi (Engl. Transl.)*, 1998, **163**, 36].
- 9 S. Cze, *VLSI Technology*, Murray Hill, New York, 1981, vol. 1, p. 620.
- 10 V. V. Azatyan, A. S. Lukashev, S. S. Nagorny, N. M. Rubtsov and S. M. Temchin, *Kinet. Katal.*, 1993, **34**, 404 [*Kinet. Catal. (Engl. Transl.)*, 1993, **34**, 351].
- 11 V. I. Chernysh, N. M. Rubtsov and G. I. Tsvetkov, *Kinet. Katal.*, 2002, **43**, 2 [*Kinet. Catal. (Engl. Transl.)*, 2002, **43**, 3].
- 12 N. M. Rubtsov, G. I. Tsvetkov and V. I. Chernysh, *Kinet. Katal.*, 2000, **41**, 340 [*Kinet. Catal. (Engl. Transl.)*, 2000, **41**, 353].
- 13 V. V. Azatyan, N. M. Rubtsov, O. T. Ryzhkov and S. M. Temchin, *Kinet. Katal.*, 1996, **37**, 805 [*Kinet. Catal. (Engl. Transl.)*, 1996, **37**, 840].
- 14 A. G. Ratnov, N. M. Rubtsov, S. M. Temchin and A. P. Dementiev, *Mikroelektronika*, 1996, **25**, 32 (in Russian).
- 15 N. M. Rubtsov, G. I. Tsvetkov, V. V. Azatyan and V. I. Chernysh, *Kinet. Katal.*, 2001, **42**, 249 [*Kinet. Catal. (Engl. Transl.)*, 2001, **42**, 286].
- 16 N. M. Rubtsov, O. T. Ryzhkov and V. I. Chernysh, *Kinet. Katal.*, 1995, **36**, 645 [*Kinet. Catal. (Engl. Transl.)*, 1995, **36**, 710].
- 17 V. V. Azatyan, A. G. Merzhanov, N. M. Rubtsov, G. I. Tsvetkov and V. I. Chernysh, *Kinet. Katal.*, 2002, **43**, 805 [*Kinet. Catal. (Engl. Transl.)*, 2002, **43**, 843].

Received: 25th April 2005; Com. 05/2500